J Mater Sci (2009) 44:4495–4498
DOI 10.1007/s10853-009-3659-5

LETTER

Nanostructuring and fluorescence properties of Eu^{3+}:$LiTaO_3$ in Li_2O–Ta_2O_5–SiO_2–Al_2O_3 glass-ceramics

Anal Tarafder · K. Annapurna · Reenamoni Saikia Chaliha · V. S. Tiwari · P. K. Gupta · Basudeb Karmakar

Received: 17 April 2009 / Accepted: 1 June 2009 / Published online: 14 June 2009

Lithium tantalate ($LiTaO_3$, LT) single crystal is one of the most important ferroelectric materials because of its unique piezoelectric, acousto-optic, electro-optic, and nonlinear optical (NLO) properties combined with good mechanical and chemical stability [1–4]. In recent years, the glasses embedded with active ferroelectric crystalline phases particularly from the perovskite family such as potassium tantalate niobate ($KTa_{0.65}Nb_{0.35}O_3$) [5], lithium niobate ($LiNbO_3$) [6], strontium titanate ($SrTiO_3$) [7], and others [8] have immense potential for a variety of applications due to their high transparency, compositional variety, low cost of fabrication, and are good alternatives to single crystal counterparts. It is observed that when activated with rare earth (RE) ions, these NLO nanocrystalline glass-ceramic composites are of considerable importance because with diode laser pumping those can lead to very compact, portable, and easy maintenance Ultraviolet (UV)–Visible laser sources [9]. In spite of its possible promising applications, work performed on nanocrystalline $LiTaO_3$ containing glass-ceramic is very limited [10]. As we are aware, there is no report so far on nanocrystalline RE^{3+}:$LiTaO_3$ containing glass-ceramics. This fact has motivated us to explore this gap. Here, we focus our attention on fluorescence characteristics of Eu^{3+}:$LiTaO_3$ transparent glass-ceramics with an emphasis on the correlation between nanocrystallite size and lifetime (τ) of dopant ion.

The precursor glass having molar composition $25.53Li_2O$–$21.53Ta_2O_5$–$35.29SiO_2$–$17.65Al_2O_3$ doped with Eu_2O_3 (0.5 wt% in excess) was prepared from high-purity Li_2CO_3, Ta_2O_5, SiO_2, Al_2O_3, and Eu_2O_3 chemicals by conventional melt-quench technique. The well-mixed raw materials were melted at 1600 °C for 2 h in air followed by quenching and annealing at 600 °C for 4 h. In the preliminary experimentation to obtain nanostructured transparent glass-ceramics in the present system, it was observed that the precursor glass had been transformed into opaque glass-ceramics after heat-treating at T_g or above T_g. In the course of this investigation, we established an optimum nucleation temperature of 650 °C and crystallization temperature of 680 °C where the nano glass-ceramics maintain their transparency. Based on these findings, we have selected the nucleation temperature of 650 °C and the heat-treatment temperature of 680 °C, which are below T_g (696 °C) of the precursor glass. Sigaev et al. [11] have also adopted a similar heat-treatment protocol for developing nanostructured transparent potassium niobium silicate glass-ceramics. For this reason, in this study, the samples were heat treated at 680 °C for 0, 1, 3, 5, 7, 10, and 20 h after nucleating at 650 °C for 2 h. The resulted glass and nano glass-ceramics were labeled as a, b, c, d, e, f, and g, respectively, for convenience. The X-ray diffraction (XRD) patterns of powdered glass and glass-ceramics were recorded using a Xpert-Pro MPD diffractometer with Anchor Scan Parameters wavelength CuK_α = 1.54060 Å at 25 °C to identify the crystalline phases. The transmission electron microscope (TEM) images and selected area electron diffraction (SAED) of powder sample were obtained from FEI (Tecnai G^2 30ST) instrument. The fluorescence emission spectra were measured on a SPEX fluorimeter (Fluorolog-II) with 150 W Xe lamp as a source

A. Tarafder · K. Annapurna · R. S. Chaliha · B. Karmakar (✉)
Glass Technology Laboratory, Central Glass and Ceramic Research Institute (CSIR), 196, Raja S.C. Mullick Road, Kolkata 700 032, India
e-mail: basudebk@cgcri.res.in

V. S. Tiwari · P. K. Gupta
Laser Materials Development and Devices Division, Raja Ramanna Center for Advanced Technology, Indore 452 013, India

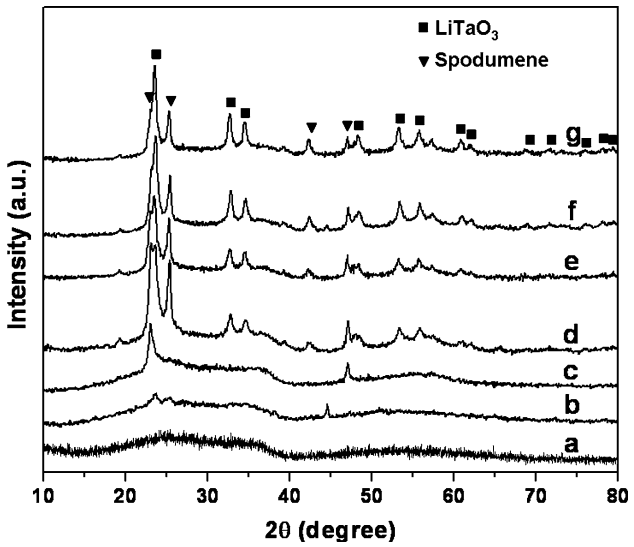

Fig. 1 XRD patterns of the samples a–g

of excitation. The fluorescence decay curves were recorded on the same instrument attached with SPEX 1934D phosphorimeter using pulsed Xe lamp.

The X-ray diffractograms of samples a–g are given in Fig. 1. The XRD pattern of the precursor glass exhibits broad humps characterizing its amorphous structure while those of the glass-ceramic samples b–g are a superimposition of same humps with series of sharp diffraction peaks attributed to rhombohedral $LiTaO_3$ (JCPDS card file no. 29-0836) except a few diffraction peak around $2\theta =$ 23.07°, 25.42°, 44.55°, and 47.11° which are due to the formation of spodumene ($LiAlSi_2O_6$) crystal phase (JCPDS card file no. 35-0797) in minor quantity. It is clearly evidenced from the XRD analysis that the peak of $LiAlSi_2O_6$ ($2\theta = 25.42°$) is more prominent in sample d with 5 h heat-treatment and it got diminished with respect to $LiTaO_3$ phase in samples e, f, and g, indicating the stabilization of $LiTaO_3$ nanocrystallites. The XRD pattern of sample b differ due to its phase separated glassy nature and having different structure than the precursor glass (a) and 3 h heat-treated glass-ceramics (c). From the full width at half maximum (FWHM) of the intense diffraction peak (012) of $LiTaO_3$, the average crystallite size (diameter, *d*) is calculated by using the Scherrer's formula [12]. It is found to vary in the range 2–32 nm for samples b–g and increases with heat-treatment duration.

TEM images of the powder samples c and f have been presented in Fig. 2a and b, respectively. The insets represent SAED pattern of the observed crystalline phase. From these figures, it is seen that the $LiTaO_3$ nanocrystallites are nearly spheroidal, clearly visible as dark spots, and homogeneously dispersed in the residual glass matrix. The crystallite sizes from TEM images of samples c and f are found to be around 13 and 20 nm, respectively. These are in good agreement with those obtained from XRD. The presence of fine spherical rings around the central bright region in SAED patterns discloses the existence of nanocrystallites in the glassy matrix.

The fluorescence emission spectra of precursor glass (a) and Eu^{3+}:$LiTaO_3$ containing nano glass-ceramics (b–g) are recorded with an excitation at 392 nm and depicted in Fig. 3. All the spectra exhibit emissions from $^5D_0$ excited level to the ground state multiplets $^7F_{0,1,2,3,4}$ levels of Eu^{3+} ions with overall dominance of electric dipole (ED) transition $^5D_0 \rightarrow {}^7F_2$. The emission peak around 532 nm has been assigned to $^5D_1 \rightarrow {}^7F_2$ transition. The most interesting result of this study is these spectral features of $^5D_0 \rightarrow {}^7F_{1,2}$ transition which reflect the local environment of Eu^{3+} ions. Upon the heat-treatment, it is also observed that the magnetic dipole (MD) emission transitions from $^5D_0 \rightarrow {}^7F_1$ and $^5D_0 \rightarrow {}^7F_2$ (ED) in glass-ceramic samples (b–f) have displayed two and three Stark splittings, respectively, with an enhanced emission from higher excited level $^5D_1 \rightarrow {}^7F_2$ at 532 nm. These changes in emission spectra of glass-ceramics suggest the fact that the Eu^{3+} ions enter into the crystalline phase ($LiTaO_3$) thus formed. In the perovskite type $LiTaO_3$ crystals, Li^+ and Ta^{5+} occupy octahedral sites with C_3 or nearly C_{3v} point symmetry. The Eu^{3+} ion is entering into the crystal ($LiTaO_3$) and it prefers to replace Li^+ over Ta^{5+}site forming $[REO_6]^{9-}$ octahedron [9, 13–15] due to the closeness of their ionic radii ($Eu^{3+} = 0.95$ Å,

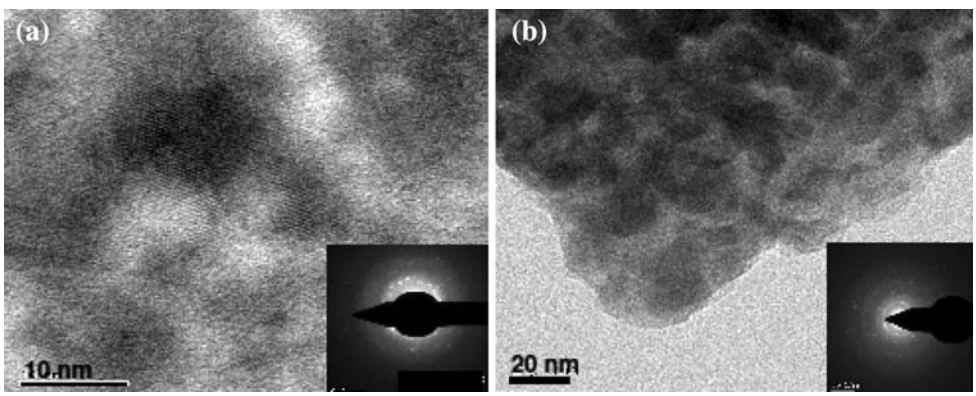

Fig. 2 TEM image and SAED (Inset) of samples: **a** c and **b** f

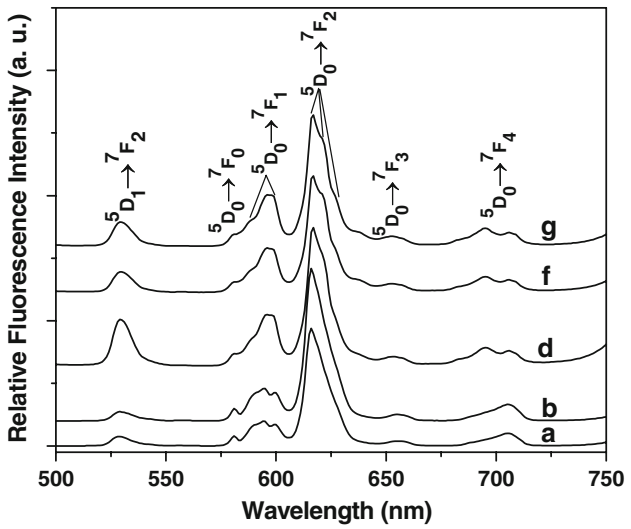

Fig. 3 Emission spectra of the samples a, b, d, f, and g under excitation at 392 nm

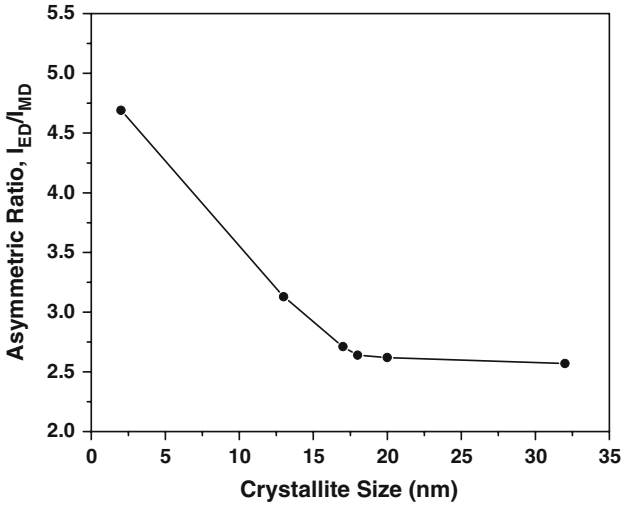

Fig. 4 Variation of asymmetric ratio (I_{ED}/I_{MD}) as a function of Eu^{3+}:$LiTaO_3$ crystallite size of the samples b–g

$Li^+ = 0.74$ Å, and $Ta^{5+} = 0.64$ Å). However, still there exists slight difference in the ionic radii between the dopant Eu^{3+} and the host Li^+ ions, consequently distorted $[EuO_6]^{9-}$ octrahedron is formed with Eu^{3+} ion facing an off-center displacement from C_3 axis in the oxygen octahedron [16, 17]. Following the crystal field selection rules, from the 2 and 3 Stark splittings, respectively, for transitions $^5D_0 \rightarrow {}^7F_{1,2}$ and from the existence of $^5D_0 \rightarrow {}^7F_0$ in the fluorescence spectra, we suggest that the rare earth (Eu^{3+}) ions are facing near C_{3v} point symmetry in its vicinity in this host matrix. As seen in Fig. 3, the $^5D_0 \rightarrow {}^7F_2$ transition is dominant in the $^5D_0 \rightarrow {}^7F_J$ transitions, and the half width for the $^5D_0 \rightarrow {}^7F_2$ transition is about 5 nm. It is, therefore, revealed from the emission spectra that the crystal field at Eu^{3+} sites in transparent nano glass-ceramics is not homogeneous. The local field asymmetry defining factor such as relative intensity ratio of ED to MD transition (I_{ED}/I_{MD}) of Eu^{3+} doped glass and glass-ceramics has been estimated from their fluorescence spectra which are plotted in Fig. 4 as a function of $LiTaO_3$ crystallite size. From this data, it is clear that, the relative intensity ratio of all samples is greater than unity, which implies that the Eu^{3+} ions take non-centrosymmetric sites. It is also noticed that the as prepared glass shows maximum value of asymmetric ratio (4.77) which has gradually been reduced in nano glass-ceramics and attained an almost saturated value at the crystallite size range 17–32 nm. This may be due to the change in bonding structure of Eu^{3+} ions with surrounding ligands in the crystalline phase compared to glassy phase as the asymmetric ratio also sensitive to degree of covalency. Thus, for longer heat treatment durations the Eu^{3+} ions are occupying the definite non-centrosymmetric sites in the well-precipitated $LiTaO_3$ crystalline phase.

The room temperature fluorescence decay curves of the emission transition ($^5D_0 \rightarrow {}^7F_2$) at 617 nm with an excitation at 392 nm for Eu^{3+} ions in as-prepared glass (a) and nano glass-ceramics (b and f) have been depicted in Fig. 5. The measured curves demonstrate a single exponential decay. The excited state ($^5D_0$) lifetime (τ) of all samples has been estimated and plotted in Fig. 6 of nano glass-ceramics as a function of $LiTaO_3$ crystallite size. The lifetime of precursor glass is estimated to be 1.185 ms. It is seen that the lifetime (τ) increases with increase in Eu^{3+}:$LiTaO_3$ nanocrystallite sizes. Such variation can be attributed to the high interaction of smaller particles with the high energy phonons of surrounding glass (about 1100 cm^{-1} of SiO_4 lattice) as revealed in the TEM image (see Fig. 2a) which increases the nonradiative relaxation with decrease in

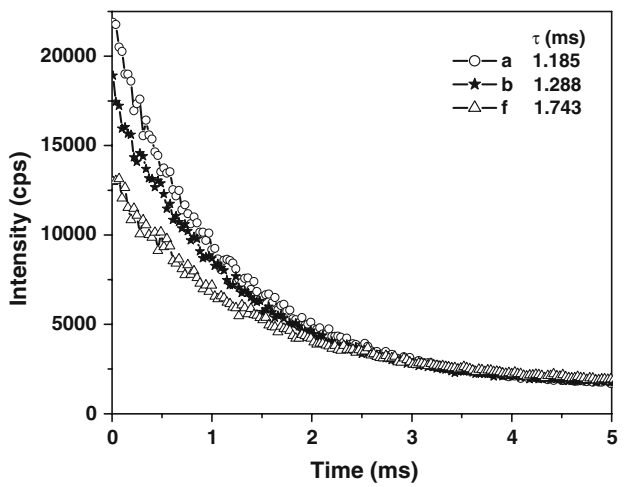

Fig. 5 Decay curves for the $^5D_0 \rightarrow {}^7F_2$ transition at 617 nm under excitation at 392 nm of the samples a, b, and f

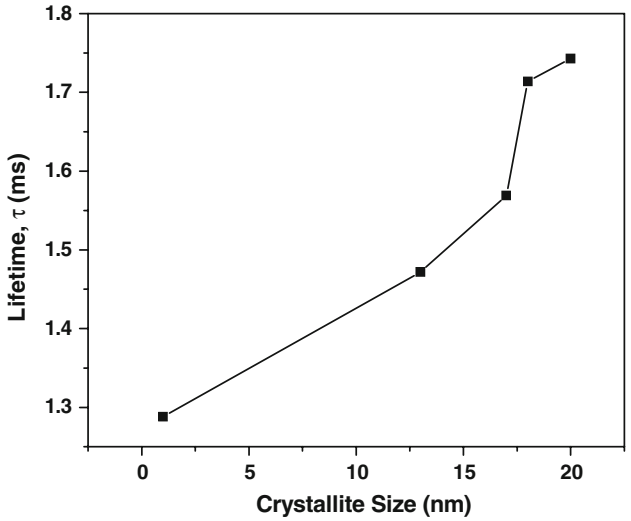

Fig. 6 Variation of excited state lifetime (τ) as a function of Eu^{3+}:$LiTaO_3$ crystallite size of the samples b–f

particle size [18]. In larger particles, less interaction with surrounding glass (see Fig. 2b) along with stable crystal site occupation by the Eu^{3+} ion in the low phonon energy $LiTaO_3$ host (about 600 cm^{-1} of TaO_6 lattice) decrease the nonradiative relaxation and thereby increase the measured lifetime (τ) as governed by the equation [19]

$$\tau = (\gamma_r + \gamma_{nr})^{-1} \quad (1)$$

where γ_r and γ_{nr} are the radiative and nonradiative rates, respectively.

In conclusion, the increase of lifetime (τ) with increase in Eu^{3+}:$LiTaO_3$ nanocrystallite size has been demonstrated in the Li_2O–Ta_2O_5–SiO_2–Al_2O_3 transparent glass-ceramics. The nanocrystallite size of $LiTaO_3$ has been evaluated from XRD and found to vary in the range 2–32 nm. This evaluation correlates well with those obtained from TEM images. In addition, the fluorescence spectra of nano glass-ceramics demonstrate that the Eu^{3+} ion has entered into the $LiTaO_3$ crystalline phase and take the nearly C_{3v} point symmetry in the place of Li^+ sites. The increase of lifetime (τ) with increase in Eu^{3+}:$LiTaO_3$ nanocrystallite size is found to be caused by the stable crystal site occupation of the Eu^{3+} ion in the low phonon energy $LiTaO_3$ host (about 600 cm^{-1} of TaO_6 lattice).

Acknowledgements This research work was supported by BRNS/DAE under the sanction No. 2007/34/05-BRNS. The authors thank Dr. H. S. Maiti, Director, CGCRI for his keen interest and kind permission to publish this paper. Electron Microscope and X-Ray Divisions of CGCRI are also thankfully acknowledged.

References

1. Naranjo B, Gimzewski JK, Putterman S (2005) Nature 434:1115
2. Abedin KS, Tsuritani T, Sato M, Ito H (1997) Appl Phys Lett 70:10
3. Zhu S, Zhu Y, Yang Z, Yang Z, Wang H, Zhang Z, Hong J, Ge C, Ming N (1995) Appl Phys Lett 67:320
4. Mizuuchi K, Yamamoto K (1995) Appl Phys Lett 66:2943
5. Lu CJ, Kuang AX (1997) J Mater Sci 32:4421. doi:10.1023/A:1018692427602
6. De Almeida EF, De Paiva JAC, Sombra ASB (2000) J Mater Sci 35:1555. doi:10.1023/A:1004765920995
7. Lu CJ, Kuang AX, Huang GY, Wang SM (1996) J Mater Sci 31:3081. doi:10.1007/BF00354652
8. Jain H (2004) Ferroelectrics 306:111
9. Romanowski WR, Sokólska I, Dzik GD, Gołab S (2000) J Alloy Compd 300–301:152
10. Ito S, Kokubo T, Tashiro M (1978) J Mater Sci 13:930. doi:10.1007/BF00544687
11. Sigaev VN, Sarkisov PD, Kupriyanova MV, Spiridonov YA, Lopatina EV, Stefanovich SY, Molev VI, Pernice P, Aronne A (2001) Glass Phys Chem 27:497
12. Cullity BD (1978) Elements of X-ray diffraction, 2nd edn. Addison-Wesley Publishing Co, London, p 101
13. Yi WS, Chen ZW (2002) Phys Rev B 65:224107
14. Wu SY, Dong HN (2005) J Alloy Compd 386:52
15. Chang YM, Yeom TH, Yeung YY, Rudowicz C (1993) J Phys C Condens Mater 5:6221
16. Milori DMBP, Moraes IJ, Hernandes AC, de Souza RR, Li MS, Terrile MC (1995) Phys Rev B 51:3206
17. Xia ZC, Yu KX, Jie MA, Hui W (2008) Physica B 403:3114
18. Meltzer RS, Yen WM, Zheng H, Feofilov SP, Dejneka MJ (2002) Phys Rev B 66:224202
19. Reisfeld R, Jørgensen CK (1977) Lasers and excited states of rare earths. Springer-Verlag, Berlin, p 98